



Contents lists available at ScienceDirect

# Bioorganic & Medicinal Chemistry Letters

journal homepage: [www.elsevier.com/locate/bmcl](http://www.elsevier.com/locate/bmcl)



## Potent and cellularly active 4-aminoimidazole inhibitors of cyclin-dependent kinase 5/p25 for the treatment of Alzheimer's disease

Christopher J. Helal<sup>a,\*</sup>, Zhijun Kang<sup>a</sup>, John C. Lucas<sup>a</sup>, Thomas Gant<sup>a</sup>, Michael K. Ahljianian<sup>b</sup>, Joel B. Schachter<sup>b</sup>, Karl E. G. Richter<sup>b</sup>, James M. Cook<sup>b</sup>, Frank S. Menniti<sup>b</sup>, Kristin Kelly<sup>b</sup>, Scot Mente<sup>c</sup>, Jay Pandit<sup>d</sup>, Natalie Hosea<sup>e</sup>

<sup>a</sup>Neuroscience Medicinal Chemistry, Pfizer Global Research and Development, Eastern Point Road, Groton, CT 06340, USA

<sup>b</sup>Neuroscience Biology, Pfizer Global Research and Development, Eastern Point Road, Groton, CT 06340, USA

<sup>c</sup>Computational Chemistry, Pfizer Global Research and Development, Eastern Point Road, Groton, CT 06340, USA

<sup>d</sup>Structural Biology, Pfizer Global Research and Development, Eastern Point Road, Groton, CT 06340, USA

<sup>e</sup>Pharmacokinetics and Drug Metabolism, Pfizer Global Research and Development, Eastern Point Road, Groton, CT 06340, USA

### ARTICLE INFO

#### Article history:

Received 10 June 2009

Revised 31 July 2009

Accepted 4 August 2009

Available online 8 August 2009

#### Keywords:

Cyclin-dependent kinase 5

p25

Cyclin-dependent kinase 2

Alzheimer's disease

### ABSTRACT

Utilizing structure-based drug design, a 4-aminoimidazole heterocyclic core was synthesized as a replacement for a 2-aminothiazole due to potential metabolically mediated toxicity. The synthetic route utilized allowed for ready synthesis of 1-substituted-4-aminoimidazoles. SAR exploration resulted in the identification of a novel *cis*-substituted cyclobutyl group that gave improved enzyme and cellular potency against cdk5/p25 with up to 30-fold selectivity over cdk2/cyclin E.

© 2009 Elsevier Ltd. All rights reserved.

Cyclin dependent kinases (cdk) carry out critical roles in cell cycling, and cdk inhibitors have been extensively researched as therapeutic agents for the treatment of cancer.<sup>1</sup> Binding of cdk5 by the protein p35 results in kinase activation and the ability to phosphorylate the cytoskeletal stabilizing protein tau, a critical component of cell structure regulation.<sup>2</sup> The membrane-bound p35 can be proteolytically cleaved by calpain to the more stable, cytosolic p25 which has led to the hypothesis that cdk5/p25 may play an integral role in Alzheimer's disease development. The longer-lived cdk5/p25 complex is believed to over-phosphorylate tau, resulting in the formation of paired helical filaments and deposition of cytotoxic neurofibrillary tangles.<sup>3</sup> Thus, inhibition of the aberrant cdk5/p25 complex is a viable target for treating Alzheimer's disease by preventing tau hyperphosphorylation and subsequent neurofibrillary tangle formation.<sup>4</sup> In addition to being a target for Alzheimer's disease, recent evidence suggests that inhibition of cdk5 could also be relevant for the treatment of type-II diabetes, pain, and stroke, furthering interest in this enzymatic target.<sup>5,6</sup>

We reported on the optimization of potency and cdk2/cyclin E selectivity in a series of 2-aminothiazole cdk5/p25 inhibitors that

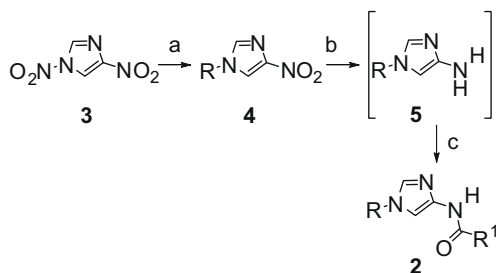
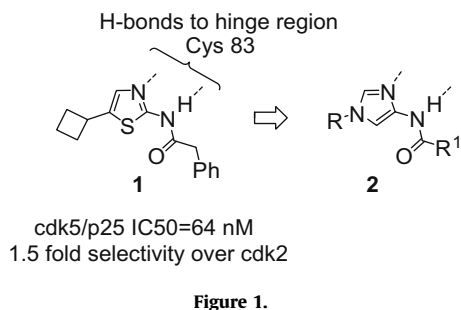
bind in the ATP binding pocket.<sup>7</sup> Selectivity over cdk2 is desired due to its role in modulating the cell cycle and potential side effects. This is a challenging task, considering 93% (27/29) of residues are conserved in the respective ATP pockets of cdk5 and cdk2 and that the two differing amino acid residues (Cys83 and Asp84 in cdk5; Leu83 and His84 in cdk2) have sidechains that project away from the ATP pocket, thereby reducing their impact on inhibitor binding.

In furthering our exploration of this series, alternative heterocyclic cores to the 2-aminothiazole (**1**) were sought, based upon the metabolism-induced toxicity potential of this class of heterocycles<sup>8</sup> (Fig. 1). Considering the binding mode of inhibitors to cdk5, as observed in computer modeling in addition to X-ray crystal structures in cdk2, key H-bond acceptor and donor interactions with Cys 83 in the hinge region (Leu 83 in cdk2) were to be maintained along with necessary lipophilic groups. The 4-aminoimidazole core (**2**) was appropriately disposed to make the requisite hydrogen bonding and hydrophobic interactions and was thus deemed a suitable target for biological evaluation.

The synthesis of 4-aminoimidazole analogs was carried out as shown in Scheme 1.<sup>9</sup> The treatment of 1,4-dinitroimidazole<sup>10</sup> (**3**) with a primary amine afforded 1-substituted 4-nitroimidazoles **4**. CAUTION: thermodynamic testing showed that **3** was a highly energetic substance with the potential for explosion.<sup>11</sup> Catalytic hydroge-

\* Corresponding author. Tel.: +1 860 715 5064.

E-mail address: [chris.j.helal@pfizer.com](mailto:chris.j.helal@pfizer.com) (C.J. Helal).



nation gave an unstable 4-aminoimidazole **5** that, following filtration through Celite, was immediately acylated with an activated carboxylic acid to afford compounds of formula **2**.

Extensive SAR of the amide side chain (not shown) revealed that the aryl acetamides were the most potent substituents. As shown in Table 1, phenylacetamide **6** was ca. eightfold less potent than the corresponding aminothiazole **1**.<sup>12</sup> Addition of a 4-methoxy group increased potency ca. fourfold (**7**). The 1-naphthyl acetamide **8** afforded the best potency with IC<sub>50</sub> = 46 nM. Activity against cdk2 was essentially equivalent to cdk5 activity.

The ability to readily synthesize *N*-1 group analogs as shown in Scheme 1 allowed for a rapid and broad exploration of SAR at this position (Table 2). The role of the *N*-1 group is critical as methyl **9** was inactive. Isopropyl analog **10** and cyclopropyl analog **11** showed improved activity, whereas cyclobutyl **7** and cyclopentyl **12** were preferred groups with IC<sub>50</sub> <200 nM. Cyclohexyl **13** lost activity as compared to **7** and **12**, as did benzyl **14**. Compound **7** was subsequently profiled for selectivity against 20 diverse kinases at 10 μM and showed >30% inhibition against three (GSK3β, 34%; AMPK, 48%; PHK, 32%).<sup>13</sup>

At this point, modeling of the cyclobutyl derivative **7** in a cdk5 homology model based upon a cdk2 X-ray crystal structure sug-

gested that placement of polar functionality on the 3-position of the cyclobutyl of **7** could possibly lead to interactions with polar amino acid side chains, Lys33 and Asp144 (Asp145 in cdk2), that interact with the phosphates of bound ATP.<sup>14</sup> These analogs were synthesized via methods that have been previously described in detail.<sup>15</sup>

The initial polar group employed was hydroxyl (Table 3, **15** and **16**). A significant effect of stereochemistry was observed with *cis*-derivative **15** being ca. 10-fold more potent than *trans* **16**, but with similar potency to the unsubstituted cyclobutyl analog **7**. A similar *cis/trans* preference was observed with the methyl esters **17** and **18**. An X-ray crystal structure of **15** bound to cdk2 was obtained (Fig. 2).<sup>16</sup> Key observations were that the cyclobutyl appears to align with Phe80, resulting in a hydrophobic interaction that explains the observed SAR. Additionally, the hydroxyl group is in position to make a hydrogen bond with Asp145 (2.7 Å) (Asp144 in cdk5), and is in proximity (3.4 Å) to Lys33. Equivalent cdk5 potency of **15** as the unsubstituted cyclobutyl analog **7** suggests that the hydroxyl interaction is energetically neutral, potentially due to desolvation penalties as a result of removing waters associated with the polar hydroxyl group, the Lys33 and/or Asp144, or with energetic loss associated with disrupting a favorable salt bridge between Lys33 and Asp144.

We thus sought to identify other possible polar groups to forge interactions with Lys33 and/or Asp144 that would afford increased potency through enthalpic contributions. The *N*-acetyl analog **19** gave a 10-fold potency increase (IC<sub>50</sub> = 9 nM) relative to **15** and also showed sevenfold greater potency for cdk5 than cdk2, demonstrating that productive interactions were in fact being made. *N*-methylsulfonyl derivative **20** maintained a similar potency preference for cdk5 over cdk2 (sixfold), but cdk5 potency dropped off considerably (IC<sub>50</sub> = 178 nM) compared to **19**. With the 1-naphthyl acetamide on the 4-aminoimidazole, *N*-acetyl analog **21** had similar potency (IC<sub>50</sub> = 8 nM) to **19** and was more selective for cdk5 over cdk2 (17-fold). The placement of polar oxygen and nitrogen atoms was demonstrated to be critical as the reversed amide **22** lost significant cdk5 potency (IC<sub>50</sub> = 391 nM) and selectivity over cdk2 (twofold). Interestingly, the *N*-methyl-*N*-acetyl analog **23** lost cdk5 potency (IC<sub>50</sub> = 107 nM), but maintained a preference for cdk5 potency over cdk2 (15-fold). Importantly, this indicates that the amide carbonyl was a primary contributor to selectivity and the amide *N*-H contributed more to potency. Compound **19** was profiled against a panel of 49 kinases and was found to inhibit four >30% at 10 μM. Subsequent profiling against these four kinases was carried out at 1 μM to ascertain potency at lower doses; GSK3β (100% @ 10 μM, 94% @ 1 μM), MAPK1/ERK2 (89%, 47%), CK1-δ (39%, 7%), CDK2/Cyclin A (101%, 94%), and CLK1 (92%, 55%).<sup>17</sup> In particular, the significant increase in potency for GSK3β activity is striking with the addition of the acetyl group in **19** as compared to the unsubstituted cyclobutyl analog **7** (94% @ 1 μM vs 34% @

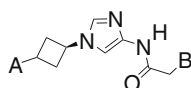
**Table 1**  
SAR of 4-*N*-acyl group

	R <sup>1</sup>	cdk5 IC <sub>50</sub> nM (std dev)
<b>6</b>	$\text{--CH}_2\text{Ph}$	500
<b>7</b>	$\text{--CH}_2\text{--4-MeOPh}$	145 (8)
<b>8</b>	$\text{--CH}_2\text{--1-Naphthyl}$	46 (18)

**Table 2**  
SAR of *N*-1 substituent

	R	cdk5 IC <sub>50</sub> nM (std dev)
<b>9</b>	Me	>10,000
<b>10</b>	<i>i</i> -Pr	425
<b>11</b>	<i>c</i> -Pr	814 (161)
<b>7</b>	<i>c</i> -Bu	145 (8)
<b>12</b>	<i>c</i> -Pentyl	154 (27)
<b>13</b>	<i>c</i> -Hexyl	748 (192)
<b>14</b>	Benzyl	8640 (1490)

**Table 3**  
SAR of cyclobutyl 3-substituent



	A	<i>cis</i> (c) <i>trans</i> (t)	B	cdk5 IC <sub>50</sub> nM (std dev)	Select <sup>a</sup> (K2/K5)
15	HO-	c	PMP	95 (42)	0.7
16	HO-	t	PMP	1090 (516)	0.7
17	MeO <sub>2</sub> C-	c	PMP	145 (57)	0.7
18	MeO <sub>2</sub> C-	t	PMP	4380 (247)	0.2
19	HN-	c	PMP	9 (8)	7
20	HN-	c	PMP	178 (46)	6
21	HN-	c	1-Naph	8 (3)	17
22	H <sub>2</sub> N(O)C-	c	1-Naph	391 (118)	2
23	N-	c	1-Naph	107 (6)	15

PMP = *para*-methoxyphenyl; 1-naph = 1-naphthyl.

<sup>a</sup> Select = ratio of cdk2 IC<sub>50</sub>/cdk5 IC<sub>50</sub>.

10 μM). Considering the potential role of GSK3β in tau phosphorylation and thus Alzheimer's disease, the ability to combine both cdk5/p25 and GSK3β inhibition into a single molecule could allow for enhanced efficacy in treating disease.<sup>18</sup>

*N*-Acetyl analog **19** was crystallized with cdk2 in order to determine key interactions and better understand the increased selectivity for cdk5 over cdk2 (Fig. 3). The amide carbonyl appears to accept a hydrogen bond from Lys33 (3.1 Å), which has shifted 1.6 angstroms relative to Figure 2. Additionally, the amide carbonyl interacts with a water molecule (2.7 Å) that bridges to the NH of Asp145. The acetyl NH is making a hydrogen bond to a water molecule, but that water is not clearly in position to bind to the protein and may thus be a crystallographic artifact.

Lys33 and Asp145 are positioned in a region of both cdk2 and cdk5 (ASP 144) where ATP phosphate binding and thus phosphorylation substrate binding happen. In cdk2 X-ray crystal structures, disorder has been observed in this region of the protein, suggesting the existence of some flexibility to accommodate the native substrate, which has been corroborated by the difference in Lys33 positioning. Thus, one hypothesis regarding preferential cdk5 inhibition versus cdk2 is that subtle differences exist between the two kinases in this flexible ATP/substrate binding region that are exploited by compounds such as **19** and **21**.

With the advent of increased selectivity and potency, further SAR exploration via modification of the cyclobutyl amide was car-

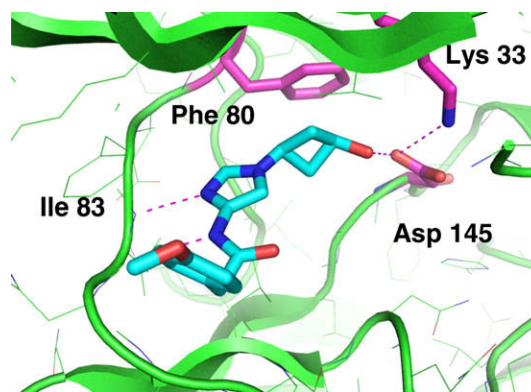


**Figure 2.** X-ray crystal structure of **15** bound to cdk2. The aminoimidazole core makes hydrogen-bonds (indicated by dashed lines) with Ile 83 in the hinge region.

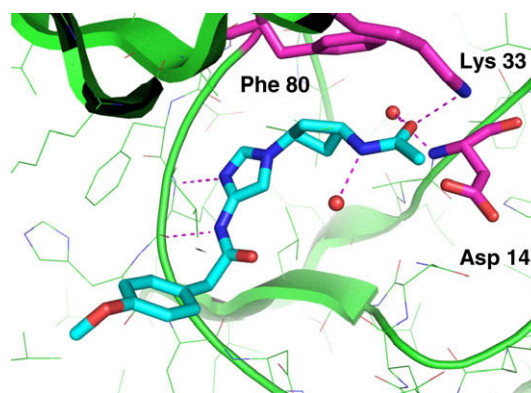


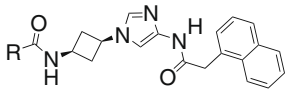
**Figure 3.** X-ray crystal structure of **19** bound to the ATP binding site of cdk2. Dashed lines indicate hydrogen bonds.

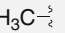
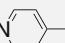
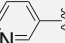
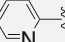
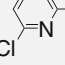
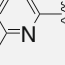
ried out (Table 4). In addition to cdk5 enzyme inhibition and selectivity for cdk5 over cdk2, inhibition of cellular cdk5/p25-mediated tau phosphorylation was measured.<sup>19</sup>

The *N*-acetyl analog **21** showed a >1000-fold loss in whole cell activity versus enzyme activity. Determination of permeability in Caco-2 cells showed significant asymmetry between the BA Papp (17.5 × 10<sup>-6</sup> cm/s) and AB Papp (1.5 × 10<sup>-6</sup> cm/s), suggestive of impaired membrane permeability. While a reduction in whole cell activity was expected, based upon the higher ATP concentration in cells than in the enzyme inhibition assay, it was hoped that a reduced shift in activity could be realized with improved permeability. In a particular sub-series of interest, the 4- and 3-pyridyl derivatives (**24** and **25**, respectively) were less active than the 2-pyridyl derivative **26** in the whole cell assay. The Caco-2 profile of **26**, with BA Papp = 21 × 10<sup>-6</sup> cm/s and AB = 26 × 10<sup>-6</sup> cm/s, was indicative of the relation between permeability and whole cell activity. The 6-chloro pyridine **27** gave improved enzyme potency (IC<sub>50</sub> = 6 nM), cdk5 selectivity over cdk2 (34-fold), and more potent whole cell activity (IC<sub>50</sub> = 673 nM) with an improved ratio of whole cell/enzyme activity (ca. 100-fold). The 6-methyl derivative **28**<sup>20</sup> had similar enzyme activity, an 18-fold preference for cdk5 versus cdk2, and the best whole cell activity (IC<sub>50</sub> = 230 nM) with a whole cell/enzyme ratio of 38. The Caco-2 profile was also good with BA Papp = 14 × 10<sup>-6</sup> cm/s and AB Papp = 13.9 × 10<sup>-6</sup> cm/s.

Compound **28** was evaluated for brain penetration in both wild-type FV/B mice and MDR1A/1B knockout mice that lack the p-glycoprotein transporter (Table 5).<sup>21</sup> In wild-type mice, brain/plasma = 0.12, whereas an order of magnitude increase in brain/

**Table 4**  
cdk5 enzyme and whole cell potency, and cdk2 selectivity



	R	cdk5 IC <sub>50</sub> nM (std dev)	Select <sup>a</sup> (K2/K5)	cdk5 whole cell IC <sub>50</sub> nM (std dev)
21	H <sub>3</sub> C- 	8 (3)	17	>30,000
24		28 (5)	11	—
25		46 (14)	15	>30,000
26		14 (9)	20	1300
27		6 (1.8)	34	673 (321)
28		6 (2)	18	230 (98)

<sup>a</sup> Select = ratio of cdk2 IC<sub>50</sub>/cdk5 IC<sub>50</sub>.

**Table 5**  
In vivo exposure for **28** at 1 h in FV/B wild-type (WT) and MDR1A/1B knockout mice<sup>a</sup>

	FV/B WT	MDR1A/B KO
Dose (mg/kg)	2	2
Plasma (ng/mL)	280	336
Brain (ng/g)	34	383
Brain/plasma	0.12	1.1

<sup>a</sup> Subcutaneous dosing; vehicle = 10% DMSO, 10% Emulphor, 80% saline.

plasma to 1.1 was observed in the MDR1A/B knockout mice. This result shows that **28** is a substrate for p-glycoprotein<sup>22</sup> with limited brain penetration in mouse and highlights the challenges of generating potent, cellularly active kinase inhibitors that can readily enter brain.<sup>18c</sup>

In summary, we have developed a novel series of 4-aminoimidazole cdk5/p25 inhibitors with potent enzyme and good whole cell activity, with good permeability in Caco-2 cell lines. Utilizing structure-based drug design, the systematic effort to build interactions with Lys 33 and Asp144, residues that are involved in binding to the ATP phosphates and thus in close proximity to substrate binding, has resulted in up to 30-fold selectivity for cdk5 over cdk2. This serves to demonstrate that selectivity is in fact possible for cdk5 over cdk2. Concurrently, we have initial data to suggest that this strategy also increases inhibition of GSK3 $\beta$ , a related tau kinase, thus potentially providing an opportunity to merge two key tau kinase inhibitory profiles into one molecule. As shown in this study, the preparation of cellularly active and selective kinase inhibitors with acceptable brain penetration remains a challenge for the field of medicinal chemistry and demonstrates a continued need for novel design strategies to access centrally located biological targets.

## Supplementary data

Supplementary data associated with this article can be found, in the online version, at doi:10.1016/j.bmcl.2009.08.019.

## References and notes

- McInnes, C. *Drug Discovery Today* **2008**, *13*, 875.
- Lau, L.-F.; Schachter, J. B.; Seymour, P. A.; Sanner, M. A. *Curr. Top. Med. Chem.* **2002**, *2*, 395.
- Lau, L.-F.; Seymour, P. A.; Sanner, M. A.; Schachter, J. B. *J. Mol. Neurosci.* **2002**, *19*, 267.
- (a) Cruz, J. C.; Tsai, L.-H. *Trends Mol. Med.* **2004**, *10*, 452; (b) Churcher, I. *Curr. Top. Med. Chem.* **2006**, *6*, 579.
- (a) Wei, F.-Y.; Tomizawa, K. *Mini-Rev. Med. Chem.* **2007**, *7*, 1070; (b) Pareek, T. K.; Kulkarni, A. B. *Cell Cycle* **2006**, *5*, 585; (c) Slevin, M.; Krupinski, J. *Curr. Opin. Pharmacol.* **2009**, *9*, 119.
- For recent reviews of cdk5/p25 inhibitors, see: (a) Glicksman, M. A.; Cuny, G. D.; Liu, M.; Dobson, B.; Auerbach, K.; Stein, R. L.; Kosik, K. S. *Curr. Alzheimer Res.* **2007**, *4*, 547; (b) Sridhar, J.; Akula, N.; Pattabiraman, N. *AAPS J.* **2006**, *8*, Article 25.
- Helal, C. J.; Sanner, M. A.; Cooper, C. B.; Gant, T.; Adam, M.; Lucas, J. C.; Kang, Z.; Kupchinsky, S.; Ahljanian, M. K.; Tate, B.; Menniti, F. S.; Kelly, K.; Peterson, M. *Bioorg. Med. Chem. Lett.* **2004**, *14*, 5521.
- Kalgutkar, A. S.; Driscoll, J.; Zhao, S. X.; Walker, G. S.; Shepard, R. M.; Soglia, J. R.; Atherton, J.; Yu, L.; Mutlib, A. E.; Munchhof, M. J.; Reiter, L. A.; Jones, C. S.; Doty, J. L.; Trevena, K. A.; Shaffer, C. L.; Ripp, S. L. *Chem. Res. Toxicol.* **2007**, *20*, 1954.
- For synthesis details, see [Supplementary data](#) and Ahljanian, M. K.; Cooper, C. B.; Helal, C. J.; Lau, L.-F.; Menniti, F. S.; Sanner, M. A.; Seymour, P. A.; Villalobos, A. WO 2002010141 A1; *Chem. Abstr.* **2002**, 107322.
- Bulusu, S.; Damavarapu, R.; Autera, J. R.; Behrens, R., Jr.; Minier, L. M.; Villanueva, J.; Jayasuriya, K.; Axenrod, T. *J. Phys. Chem.* **1995**, *99*, 5009.
- Thermodynamic testing showed that **3** was a highly energetic substance with the potential for self-heating from 35 °C that could lead to explosion. This material should be used in small amounts and stored in a freezer. Solutions of **3** in methanol (1 M or less) were found to have reduced explosive potential and thus reactions at 23 °C were deemed to be of reduced risk. Nonetheless, appropriate safety procedures should be strictly observed when handling this compound.
- Kinase inhibition was measured by the use of scintillation proximity assays (SPA). The ATP final concentration of about 0.5  $\mu$ M was the same in both the cdk5/p25 and cdk2/cyclin E assay. The  $K_m$  of ATP was measured to be 12  $\mu$ M for cdk5/p25 and 19  $\mu$ M for cdk2/cyclin E. Unless otherwise indicated, for compounds with IC<sub>50</sub> < 1  $\mu$ M, the IC<sub>50</sub>s reported are the mean of at least two independent measurements with standard deviation (std dev) calculated. Each IC<sub>50</sub> was determined from a six-point dose-response curve run in triplicate.
- Compound **7** was profiled against the following 20 kinases at a concentration of 10  $\mu$ M and [ATP] at  $K_m$  for the respective kinase: MKK1, JNK, p38, p38 $\alpha$ , p38 $\gamma$ , p38 $\delta$ , MAPKAP-K2, MSK1, PKC $\alpha$ , PDK1, PKB $\alpha$ , SGK, P70S6K, GSK3 $\beta$ , ROCKII, AMPK, CK2, MAPKAP-K1b, MAPK1, PHK.
- The cdk5 homology model was built on in-house X-ray structures of cdk2-inhibitor complexes, and due to the high homology between the two, is very similar to the cdk2 X-ray structures themselves. Retrospectively, comparing the homology model to that of the reported cdk5-inhibitor complexes (Mapelli, M.; Massimiliano, L.; Crovace, C.; Seeliger, M. A.; Tsai, L.-H.; Meijer, L.; Musacchio, A. *J. Med. Chem.*, **2005**, *48*, 671) reveals nearly identical residue-by-residue similarity.
- (a) Helal, C. J.; Kang, Z. K.; Lucas, J. C.; Bohall, B. R. *Org. Lett.* **2004**, *6*, 1853; (b) See [Supplementary data](#) for representative experimental conditions, yields, and spectral data.
- (a) Human recombinant cdk2 was expressed, purified and crystallized as described previously (Brown, N. R.; Noble, M. E.; Lawrie, A. M.; Morris, M. C.; Tunnah, P.; Divita, G.; Johnson, L. N.; Endicott, J. A. *J. Biol. Chem.* **1999**, *274*, 8746). Structures were derived from cdk2 crystals that were soaked in solutions containing inhibitor; (b) The X-ray crystal structures have been placed in the PDB with code numbers 3IGG (Fig. 2) and 3IG7 (Fig. 3).
- Compound **19** was profiled against the following 49 kinases with [ATP] =  $K_m$  for the respective kinase: ABL, CK1 $\delta$ , GSK3 $\beta$ , IKK1, IKK $\beta$ , LCK, MAPKAP-K2, p38 $\alpha$ , PKA, PKC $\epsilon$ , CDK2/Cyclin A, CHK1, CHK2, FGFR1, MET, PAK4, PDK1, PIM2, SRC, CK-II, EGFR, TRK-A, VEGFR-2, AKT1, INSR, Aurora-A, MAPK1/ERK2, SGK, BTK, TAOK3, CAMK1, ECK, PKC $\beta$ , CLK1, MARK1, NEK2, JAK3, MYLK2, MAP3K9, MASK, S6K-T389E-D3E, ROCK1, SYK, MST2, CDK6/Cyclin D3, MAP4K4, MEK1, TGFR-1, BRAF.
- (a) Gong, C.-X.; Iqbal, K. *Curr. Med. Chem.* **2008**, *15*, 2321; (b) Engmann, O.; Giese, K. P. *Front. Mol. Neurosci.* **2009**, *2*, 2; (c) Mazanetx, M. P.; Fischer, P. M. *Nat. Rev. Drug Discovery* **2007**, *6*, 464.
- cdk5 whole cell assay: A tetracycline-regulated expression system was used to produce a stable CHO cell line carrying inducible expression of human Cdk5, P25 and tau driven from modified pRevTRE Tet-Off vectors containing distinct antibiotic resistance genes. The cell line was maintained in the uninduced state in media containing doxycycline and then transgene induction was initiated by removal of doxycycline from the medium for 24 h. Following full induction of CDK5, P25, and tau, cells were incubated for 2 h with test compounds before lysis. Phosphorylated tau was measured in detergent-soluble extracts of cells using AlphaLISA (Perkin-Elmer). A capture antibody to total tau (HT7, Pierce) was conjugated to Acceptor beads, and a biotinylated phospho-epitope specific detection antibody (AT8, Pierce) was bound to streptavidin donor beads (Perkin-Elmer).

20. Compound **28** characterization data:  $^1\text{H}$  NMR (400 MHz,  $\text{CDCl}_3$ )  $\delta$  9.15 (s, 1H), 8.28 (d,  $J = 8.3$  Hz, 1H), 8.01 (d,  $J = 7.5$  Hz, 1H), 7.97 (d,  $J = 7.5$  Hz, 1H), 7.96 (d,  $J = 7.5$  Hz, 1H), 7.81 (dd,  $J = 2.4, 6.6$  Hz, 1H), 7.72 (m, 1H), 7.5 (m, 5H), 7.2 (m, 1H), 7.16 (s, 1H), 4.45 (m, 1H), 4.25 (m, 1H), 4.18 (s, 2H), 2.98 (m, 2H), 2.60 (s, 3H), 2.40 (m, 2H); MS (AP/CI): 440.3 ( $\text{M}+\text{H}$ ) $^+$ .
21. Shinkel, A. H.; Wagenaar, E.; Mol, C. A.; van Deemter, L. J. *Clin. Invest.* **1996**, 97, 2517.
22. For an analysis of commercial drugs' brain penetration in wild type versus MDR1A/1B knockout mice, see: Doran, A. et al *Drug Metab. Dispos.* **2005**, 33, 165.